Visions and Strategies for Reinforcing Additively Manufactured Constructions 2023

Conference paper

https://doi.org/10.52825/ocp.v3i.227

Published: 15 Dec. 2023

Enclosing Reinforcement Structures in Shotcrete 3D Printing

The Effect of Reinforcement Geometry and Accelerator Dosage on the Formation of the Bond Area

Niklas Freund[1] [https://orcid.org/0000-0003-2392-5439], Robin Dörrie[2] [https://orcid.org/0000-0001-8473-7218], Martin David[3] [https://orcid.org/0000-0001-5386-4855], Harald Kloft[2] [https://orcid.org/0000-0003-4891-869X], Klaus Dröder[3] [https://orcid.org/0000-0002-6424-4384], and Dirk Lowke[1,4] [https://orcid.org/0000-0001-8626-918X]

[1] Institute of Building Materials, Concrete Construction and Fire Safety (iBMB), Technische Universität Braunschweig, Germany

[2] Institute of Structural Design (ITE), Technische Universität Braunschweig, Germany

[3] Institute of Machine Tools and Production Technology (IWF), Technische Universität Braunschweig, Germany

[4] Department of Materials Engineering, Technical University of Munich, Germany

Abstract. Integrating reinforcement into existing concrete 3D printing processes represents one of the key challenges in further automating the additive manufacturing of structural concrete components. Several different reinforcing approaches are currently being investigated. In this context, the Short Rebar Insertion (SRI), as well as the use of prefabricated reinforcement structures, are potential strategies. A common feature of both methods is that rebars protrude from the already printed concrete in different orientations during the printing process and must be embedded in the subsequent concrete layers. Due to the spray application, Shotcrete 3D Printing (SC3DP) offers a good basis for realizing such reinforcement enclosures without the need for specially adapted nozzles, as often used in material extrusion. However, it is essential to systematically analyze the effect of reinforcement properties, such as reinforcement orientation, and material properties, such as accelerator dosage, to define the application boundaries. For this reason, the present study investigates the enclosing of different reinforcement geometries (spacing, inclination, crossings) with unaccelerated and accelerated fine-grained concrete to evaluate the enclosing process. It is shown that all centrally positioned reinforcement structures could be homogeneously enclosed in the SC3DP process. However, for a small rebar spacing and for accelerated material, the eccentric reinforcement structures increasingly act as a blocking element for material spreading. Furthermore, the accumulation of concrete on the top of the reinforcement during spraying creates a shielding effect that increasingly leads to void formation. Finally, recommendations are made for the enclosure of protruding reinforcement structures in SC3DP.

Keywords: Additive Manufacturing in Construction; 3D Concrete Printing; Shotcrete 3D Printing, Protruding Rebars; Accelerator; Bond Quality; Void Formation;

Introduction

In recent years, 3D printing of concrete has been increasingly adopted by the construction industry due to the new possibilities in component design and efficient use of materials. This

can be seen in a large number of demonstration projects in the building and infrastructure sectors [1]. While the printing techniques are based on an automated fabrication process, the integration of reinforcement, which is essential for most structural elements, is often subject to manual process steps. In many cases, a lost formwork is printed into which reinforcement is incorporated and then filled with concrete [2]. Although this is the reinforcement strategy closest to existing construction methods, it minimizes geometric freedom and the automation of additive manufacturing in construction due to the necessary manual process steps. The goal of automated manufacturing must be combined processes for the production of reinforced components that combine the 3D printing of concrete and the integration of reinforcement, thus maximizing automation and efficient use of materials.

In this context, several different reinforcement strategies have been investigated. These differ in the time of integration, e.g. before, during, or after the concrete printing process, and in the integration type, e.g. integration through already printed layers, between printed layers or the enclosure of prefabricated reinforcement structures [3,4]. The aim of all reinforcement strategies is to achieve good bond quality to ensure the required mechanical performance. It has been shown that in addition to the influences of the integration process, e.g. the design of the integration, the existing fresh concrete properties, e.g. the yield stress of the material, significantly influence the resulting bond quality [5,6].

Within the Short Rebar Insertion (SRI) strategy [6], rebar integration is typically performed in two steps. The short rebars are integrated through the printed layers in the first step. This can be done either perpendicular to the layer or at an angle, see **Figure 1**a. Here, the rebars are only partially integrated so that a defined length protrudes from the concrete surface. On the one hand, this is due to the retention of the rebar end effector. On the other hand, it represents a needling of the printed sections in the sense of an increase of layer bond, which can be particularly relevant in the case of interruptions in the printing process.

Figure 1: Process steps of short rebar insertion (SRI): a) angled short rebar insertion, b) enclosing process of protruding rebars.

In the second process step, the protruding rebars are enclosed by the printing process, see **Figure 1**b. Due to printing with a defined nozzle distance and material application in a spray jet, no specially designed nozzle, such as a twin nozzle, is required in the context of Shotcrete 3D Printing (SC3DP) [7]. In addition to SRI, the characteristic of enclosing protruding rebars is also present in the reinforcement strategies of prefabricated reinforcement structures and incremental reinforcement integration. In this case, moreover, free-form and complex reinforcement structures, e.g. force-flow oriented, can be integrated into the manufacturing process [8]. In order to achieve a good bond quality for the reinforcement enclosure process, the present study will investigate the effect of reinforcement geometry and material properties on the formation of voids.

Scope and concept of investigations

This study will systematically investigate the enclosure of protruding reinforcement structures in the SC3DP process. In addition to different reinforcement geometries, the material-related

effect of using an accelerator will be investigated. The effect of the reinforcement geometry is investigated within five test fields, which include the following geometric specifications and are visualized in **Figure 2**:

- Spacing between vertical rebars increasing from 2 to 30 mm (test field 1)
- Inclination angle of the rebars increasing from 15 to 60° (test field 2)
- Spacing between single horizontal rebars and the base, e.g. prior printed concrete layers, with decreasing distances from 120 to 30 mm (test field 3)
- Spacing between two horizontal rebars among each other and towards the base with decreasing distances from 90 to 30 mm (test fields 4)
- Inclination angle of crossing rebars from 60 to 15° (test field 5)

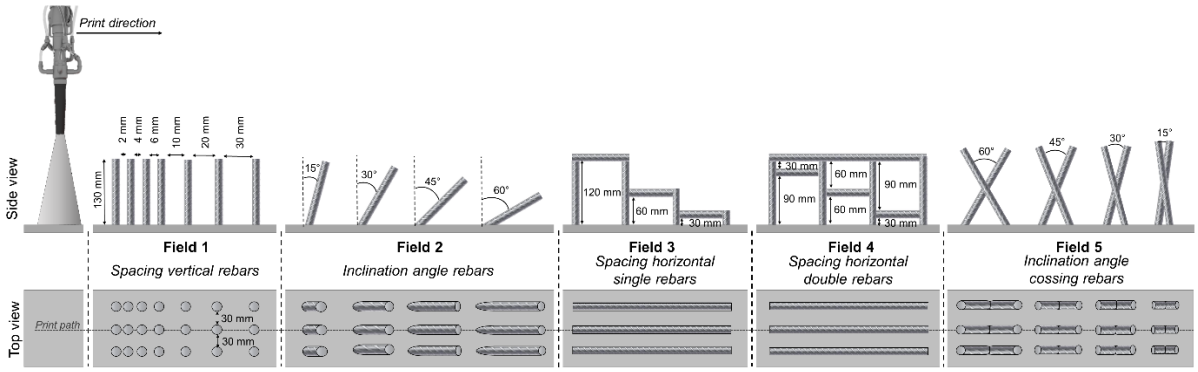

Figure 2: Schematic illustration of the test fields used.

In each test field, the reinforcement structure is positioned once centrally and eccentrically on both sides at a distance of 30 mm from the center of the jet, see **Figure 2** bottom. The following research questions are to be answered:

i. What is the effect of geometry (spacing between vertical and horizontal rebars, inclination of rebars, and crossing rebars) on the enclosure of centrally positioned reinforcement structures in the SC3DP process?
ii. How does an eccentric positioning of reinforcement structures at the edge zones of the spray jet affect the enclosure process?
iii. How does a high acceleration of the applied material affect the resulting enclosure of the reinforcement structures?

Materials and methods

Materials. A sprayable mortar with a maximum grain size of 2 mm (MC Bauchemie-Müller GmbH & Co. KG, Germany) is used in this study. For each batch, 100 kg of dry mix is mixed with 16 L of water in a pug mill mixer (Mader WM Jetmix 125/180, Germany). The mixing time was kept constant at 4 minutes. A summary of the mortar composition is given in **Table 1**. The accelerator is delivered to the SC3DP nozzle by a dosing pump and added to the compressed air at the end of the nozzle.

Table 1: Mixture composition of SC3DP material

Component	Value	Unit
Ordinary Portland Cement (CEM I 52.5 R)	500	kg/m³
Pozzolan	160	kg/m³
Silica fume	25	kg/m³
Aggregate; d=0-2 mm	1180	kg/m³
Pulverized additives and micro polypropylene fibres	33	kg/m³
Alkali-free set accelerator	0 and 6	wt.% bwoc

Preparation of reinforcement structures. Conventional 12 mm diameter rolled reinforcement bars (B500B ductile steel, according to [9]) were used to construct the reinforcement structures. The reinforcement structures were then fixed in a wooden plate for the enclosing SC3DP process, see **Figure 3**. To create the geometries of test fields 3, 4 and 5, rebars were welded together.

Figure 3: Picture of the prepared test fields 1 - 5.

Specimen preparation. All specimens were fabricated at the Digital Building Fabrication Laboratory (DBFL) [10] by using the SC3DP process [11]. The DBFL has a workspace of 10.15 m × 5.25 m × 2.5 m (W × L × H) and is equipped with two portals mounted on a 3-axis gantry system [10]. For the presented series of tests, the first portal, which carries an industrial robot (6-axis Stäubli TX200), was used. The test fields were lined up as shown in **Figure 2** and **Figure 3** so that they could be enclosed by a linear path movement. Here, the material was applied on both the forward and return movements. The nozzle-to-strand-distance was 200 mm and the traverse speed was 4500 mm/min. The concrete volume flow was 0.4 m³/h and the air volume flow was 40 m³/h. The nozzle was aligned perpendicular to the ground without an angle and the test fields were passed centrally, see **Figure 4**a. The selected process parameters resulted in a production time of approximately 5 minutes for each material setting. However, it must be noted that during the production with the accelerated material, the test field and nozzle were not ideally centered, resulting in a slightly offset material application, see **Figure 4**b.

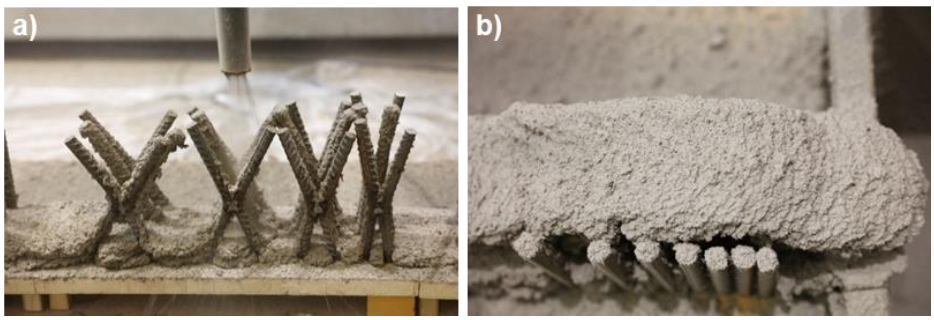

Figure 4: a) Central passing of the nozzle with a nozzle distance of 200 mm over test field 5, b) Displaced passing for accelerated material over test field 1.

Investigation of fresh concrete properties. In order to evaluate the yield stress of the printed concrete, an additional straight strand was produced with SC3DP and then sampled with a shotcrete penetrometer (according to [12]). The penetration force was measured during

the first 30 min after material application at a repetition rate of 10 measurements per time step. The measured penetration forces were then converted into yield stress according to [13].

Visual control of the printing process and resulting enclosure quality. The evaluation of the reinforcement enclosure is carried out in two steps. The first step is a visual inspection of the printing process. Attention is paid to special features, such as a defective enclosure, which can already be detected during printing. In the second step, the produced samples are analyzed for internal defects. For this purpose, the samples are cut into slices in the hardened state using a CNC-controlled gantry saw, which allows the bonding zones of the integrated reinforcement to be inspected for voids on the sawn cross-section. In order to ensure that the uneven specimens could be sawn stably without causing damage, the individual test fields were cast in molds using concrete colored with yellow pigments. At least three cuts were made for each test area to provide information on voids, i.e. at the specimens' top, middle and bottom.

Results and discussion

Fresh concrete properties. With regard to the fresh concrete properties, a clear effect of the accelerator on the resulting yield stress can be observed. The results of the penetration tests are shown in **Figure 5**. In addition to a significantly higher initial yield stress for the accelerated material, a faster increase in yield stress over time is evident, i.e. a higher structural build-up. At 0 minutes after material application, which corresponds to the initial yield stress immediately after material application, the unaccelerated material has a yield stress of 10.8 kPa and the accelerated material of 143.4 kPa. Thus, the initial material properties differ significantly when the material hits the reinforcement structure. Looking at the 5-minute time point, which is approximately the end of the printing process, a yield stress of 12.5 kPa can be measured for the unaccelerated material. In contrast, the accelerated material has a yield stress of 322.8 kPa.

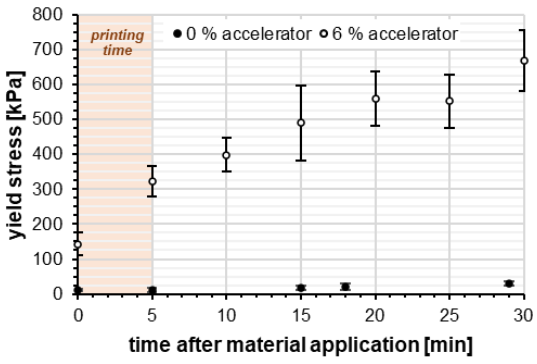

Figure 5: Evolution of the yield stress for unaccelerated and accelerated material (6 % bwoc) after material application using the SC3DP process.

Vertical and inclined rebars (field 1 & 2). The sectional views in Figure 6a show that for the unaccelerated material, a very good enclosure of the center rebars was achieved regardless of the bar spacing. A void-free enclosure was achieved even with the smallest bar spacing of 2 mm.

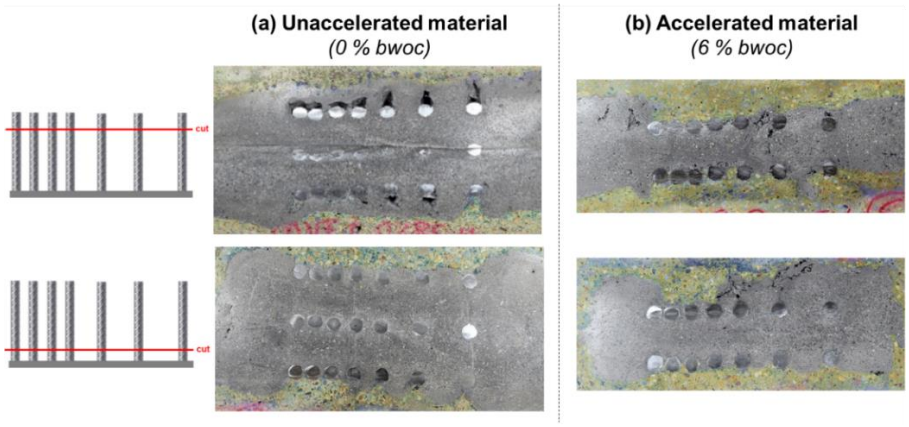

Figure 6: Sawn cross-sections at the top and bottom of test field 1 with vertical rebars, (a) unaccelerated material, (b) accelerated material.

However, for the outer rows of rebars, a lateral blocking effect is visible. Depending on its yield stress and the existing rebar spacing, the material sprayed onto the reinforcement structure is limited in its horizontal spread. This lateral blocking effect can result in two types of defects, see **Figure 7**.

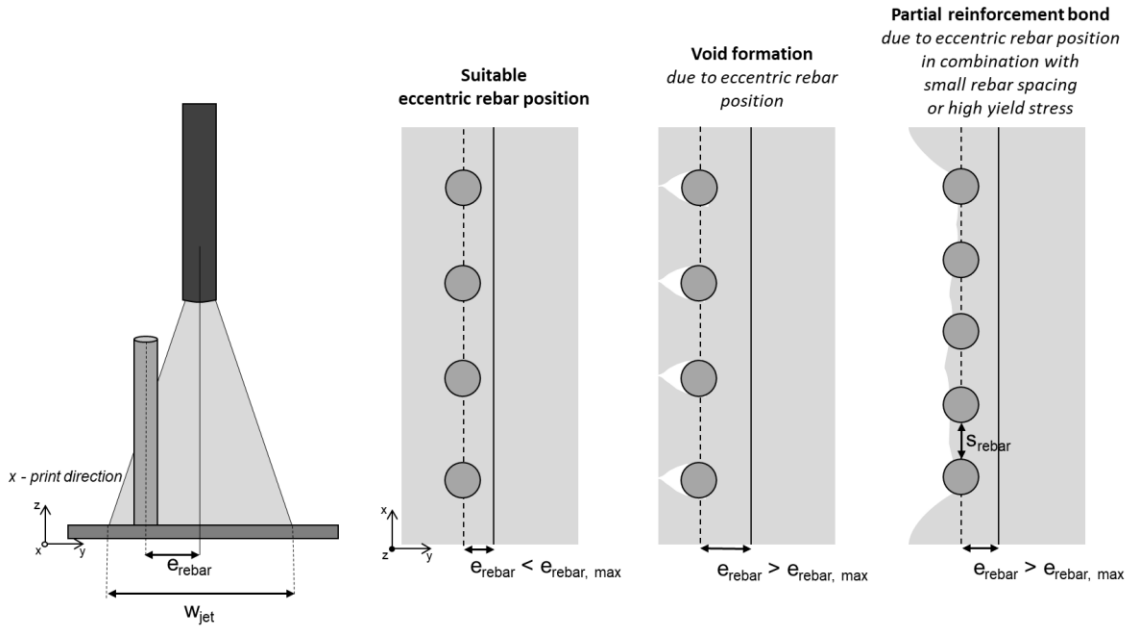

Figure 7: Eccentric distance e_{rebar} to the center of the spraying cone.

(1) Void formation behind rebars: While in the upper section, the outer rebars are partially completely enclosed when using the unaccelerated material (**Figure 6**a top), in some cases, local voids have formed on the outer sides of the rebars in the shadow area. This effect increases with increasing specimen height (compare **Figure 6**a bottom and top), which is attributed to a shielding effect of material accumulated on the reinforcement structure during printing.

(2) Partial reinforcement bond: **Figure 8**a gives a detail of test field 1, which clearly shows that the applied material is restricted to the inner area of the reinforcement. For the unaccelerated material, this phenomenon is only present for a dense rebar arrangement as in test field 1. For the test fields with a less dense reinforcement arrangement, a lateral spread

of the layers can be observed. However, for the eccentric rebars, local defects are still present laterally next to the rebars, see **Figure 8**b.

Figure 8: Lateral blocking of the unaccelerated material by reinforcement structure for a) test field 1 and b) test field 2.

Unfortunately, because the nozzle did not pass centrally over the reinforcement for the accelerated material, the material was applied mainly in the space between two rows of reinforcement, see **Figure 6**b. Therefore, no row of reinforcement was passed centrally. However, it can be seen that the lateral blocking effect is even more pronounced for the accelerated material due to the higher yield stress. As the bar spacing increases, the material flows further between the bars than when the bar spacing is small, see **Figure 6**b.

The results show that it is feasible to apply vertical and inclined reinforcement in a distributed manner across the width of the layer. However, reinforcement arranged eccentrically to the concrete jet and/or high degrees of reinforcement, i.e. low rebar spacing, can result in defects in the reinforcement bond. In order to define a maximum eccentric position $e_{rebar,max}$ to avoid the formation of defects, it is necessary to consider factors such as the jet width w_{jet}, the initial yield stress τ_0 of the sprayed concrete and the bar spacing s_{rebar}, see **Figure 7**. If it is not possible to center the concrete jet over all rebars across the width of the component, the use of two or more adjacent layers can be considered, each allowing for a centered or slightly eccentric reinforcement enclosure, see **Figure 9**a. For small bar spacings or highly protruding reinforcement structures, angled enclosures with an application angle $\alpha > 0°$ can also be used, see **Figure 9**b. For partially embedded reinforcement structures, as shown in Figure 8, a subsequent enclosure can also be achieved through cover layer printing ($\alpha = 60 – 90°$), see Figure 9c.

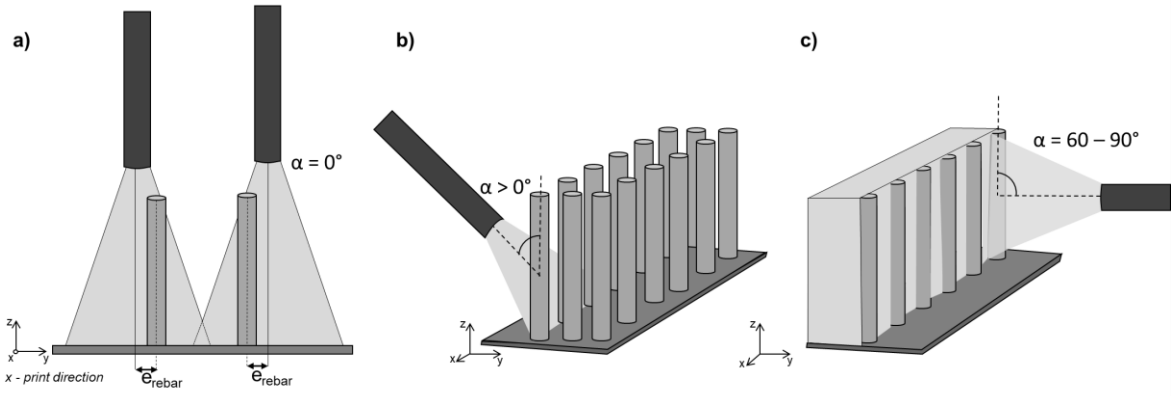

Figure 9: Concepts for path planning strategies; a) enclosure of reinforcement with two adjacent layers and straight nozzle orientation $\alpha = 0°$, b) enclosure of reinforcement with a nozzle angle $\alpha > 0°$ and c) subsequent enclosure of partially embedded rebars by cover layer printing.

Horizontal and inclined crossing rebars (field 3, 4 & 5). Again, good enclosure results were achieved for the centrally aligned reinforcement structures for horizontal and inclined crossing rebars (see Figure 10). However, for the eccentric reinforcement structures, voids were formed on the outward side of the rebars.

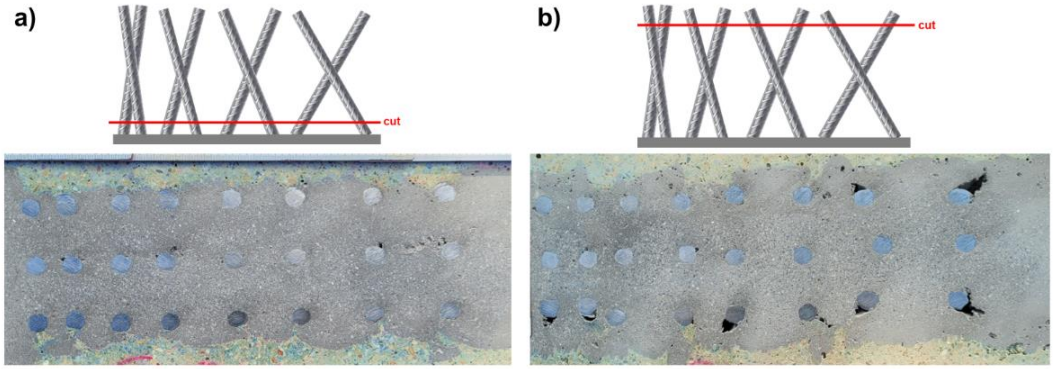

Figure 10: Increase in voids in comparison of the cross-section at the bottom and top of test field 5 with inclined crossing rebars manufactured with unaccelerated material.

Similar to the vertical rebars of test field 1 (**Figure 6**), it can be seen that the formation of these voids also increases towards the top of the reinforcement structure, see **Figure 10**b. As mentioned, this may be related to air entrapment underneath material accumulated at the top of the reinforcement structure during printing. The accumulation of material at the top of the reinforcement could be observed during the printing process for both the unaccelerated and accelerated material, see **Figure 11**a. This material acts as a shield for the area below. As the printing process continues to progress, the kinetic energy of the spray jet causes some of the accumulated material to move downwards, allowing a steady filling of the areas below the top surface.

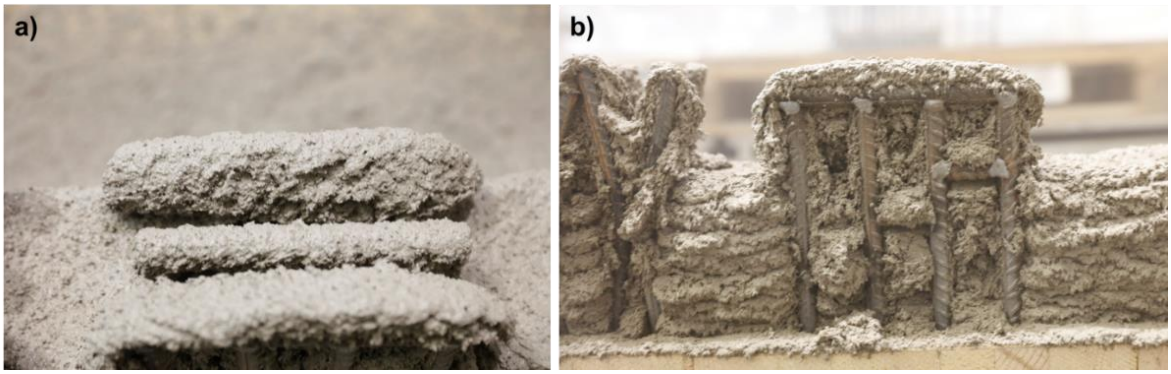

Figure 11: Accumulation of accelerated material on top of the protruding reinforcement structure; a) top view and b) side view.

However, for accelerated material and an increasingly dense reinforcement arrangement, the accumulation of material for test field 5 (crossings) results in larger voids within the reinforcement structure as the accumulated material has almost completely shielded the underlying area, see **Figure 12**. Due to the high structural build-up of the accelerated material (compare **Figure 5**), the displacement of the material by the newly applied concrete is limited, i.e. the cavities can no longer be closed entirely during the subsequent printing process.

Figure 12: Resulting large cavities in test field 5 for accelerated material due to the shielding of material accumulated on the top surface.

In order to avoid or minimize material accumulation on inclined crossing rebars, it is recommended to use a limited protrusion height. For high protrusion heights, the lateral path planning visualized in **Figure 9**b with a nozzle inclination $\alpha > 0°$ could also be used. Furthermore, as shown in [14], laterally exposed reinforcement resulting from the lateral blocking effect (see **Figure 8**) can be subsequently enclosed by a cover layer ($\alpha \approx 60 - 90°$) as part of the surface finish, see Figure 9c. However, the irregular surface, defined by cavities, results in differing volumes of material required. Consequently, employing sensor-based process monitoring and online process control is recommended [15,16].

In addition to the risk of void formation, an uneven, wavy layer surface can be observed, see **Figure 13**. Here, a denser reinforcement arrangement leads to an increasing dimension of this effect. In general, this effect is more pronounced for accelerated material than for unaccelerated material, compare **Figure 13**a and b. Therefore, a sensor-based control of the layer heights, according to [16], is recommended to be able to compensate for the resulting layer irregularities in the process.

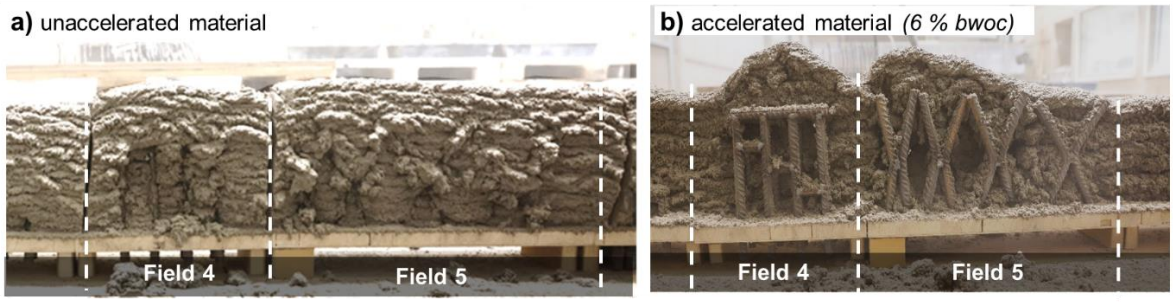

Figure 13: Uneven printed concrete surface due to underlying reinforcement structure for a) unaccelerated material and b) accelerated material.

Conclusion

This study investigated the enclosure of protruding reinforcement structures using the Shotcrete 3D Printing process. The aim was to investigate the effect of different geometric complexities as well as centric and eccentric reinforcement arrangements on void formation. The experiments were carried out using unaccelerated and highly accelerated material (6% bwoc). The following conclusions can be drawn from the study:

- Reinforcement structures centrally passed by the nozzle achieve homogeneous bond zones with unaccelerated material, regardless of the investigated geometric layouts.

- For small rebar spacings, the eccentric rebars act as a blocking element for lateral material spread. This results in either complete retention of the material or the formation of voids in the shadow area on the outer side of the rebars.
- During the printing process, material can accumulate, particularly at the top of horizontal or inclined crossing reinforcement structures, resulting in a shielding of the area below. This leads to increased void formation at the top of the reinforcement structure and the formation of a wavy layer surface.
- The addition of 6 % accelerator resulted in a significant increase in the initial yield stress and structural build-up of the material. This increases the effects of lateral blocking and material accumulation at the top of the reinforcement structures, forming large voids within the reinforcement structure.

The present study shows that SC3DP provides a good basis for the integration of protruding reinforcement structures. However, further research has to be conducted regarding the maximum protrusion lengths and the maximum eccentric positioning over the spray jet width. In addition, alternative path planning strategies, such as spraying with an inclination angle, the arrangement of two adjacent layers, or the application of a vertical cover layer, can be considered.

Data availability statement

The data that support the findings of this study were generated at the Institute of Building Materials, Concrete Construction and Fire Safety (iBMB), Division of Building Materials, Technische Universität Braunschweig (Germany) and are available on request from *baustoffe@ibmb.tu-bs.de*.

Author contributions

Conceptualization, N.F., D.L.; methodology, N.F., D.L.; validation, N.F.; formal analysis, N.F.; investigation, N.F., R.D., M.D.; resources, D.L., H.K., K.D.; data curation, N.F.; writing—original draft preparation, N.F.; writing—review and editing, N.F., R.D., M.D., H.K., K.D., D.L.; visualization, N.F.; supervision, D.L., H.K., K.D.; project administration, N.F, R.D., M.D.; funding acquisition, D.L., H.K., K.D.; All authors have read and agreed to the published version of the manuscript.

Competing interests

The authors declare no competing interests.

Funding

Funded by the Deutsche Forschungsgemeinschaft (DFG, German Research Foundation) – TRR 277/1 2020 – Project number 414265976. The authors thank the DFG for the support within the CRC/ Transregio 277 - Additive Manufacturing Construction. (Project A04).

References

1. Buswell, R.A.; Bos, F.P.; Da Silva, W.R.L.; Hack, N.; Kloft, H.; Lowke, D.; Freund, N.; Fromm, A.; Dini, E.; Wangler, T.*; et al.* Digital Fabrication with Cement-Based Materials: Process Classification and Case Studies. In *Digital Fabrication with Cement-Based Materials*; Roussel, N., Lowke, D., Eds.: Springer International Publishing: Cham, 2022, pp. 11–48, https://doi.org/10.1007/978-3-030-90535-4_2.

2. Bos, F.P.; Menna, C.; Pradena, M.; Kreiger, E.; da Silva, W.L.; Rehman, A.U.; Weger, D.; Wolfs, R.; Zhang, Y.; Ferrara, L.*; et al.* The realities of additively manufactured concrete structures in practice. *Cement and Concrete Research* **2022**, *156*, 106746, https://doi.org/10.1016/j.cemconres.2022.106746.
3. Kloft, H.; Empelmann, M.; Hack, N.; Herrmann, E.; Lowke, D. Reinforcement strategies for 3D-concrete-printing. *Civil Engineering Design* **2020**, *2*, 131–139, https://doi.org/10.1002/cend.202000022.
4. Mechtcherine, V.; Buswell, R.; Kloft, H.; Bos, F.P.; Hack, N.; Wolfs, R.; Sanjayan, J.; Nematollahi, B.; Ivaniuk, E.; Neef, T. Integrating reinforcement in digital fabrication with concrete: A review and classification framework. *Cement and Concrete Composites* **2021**, *119*, 103964, https://doi.org/10.1016/j.cemconcomp.2021.103964.
5. Freund, N.; Lowke, D. Interlayer Reinforcement in Shotcrete-3D-Printing. *Open Conf Proc* **2022**, *1*, 83–95, https://doi.org/10.52825/ocp.v1i.72.
6. Freund, N.; Dressler, I.; Lowke, D. Studying the Bond Properties of Vertical Integrated Short Reinforcement in the Shotcrete 3D Printing Process. In *Second RILEM International Conference on Concrete and Digital Fabrication*; Bos, F.P., Lucas, S.S., Wolfs, R.J., Salet, T.A., Eds.: Springer International Publishing: Cham, 2020, pp. 612–621, https://doi.org/10.1007/978-3-030-49916-7_62.
7. Kloft, H.; Empelmann, M.; Oettel, V.; Ledderose, L. 3D Concrete Printing – Production of first 3D Printed Concrete Columns and Reinforced Concrete Columns. *BFT International, no. 6* **2020**, 28–37.
8. Dörrie, R.; Laghi, V.; Arrè, L.; Kienbaum, G.; Babovic, N.; Hack, N.; Kloft, H. Combined Additive Manufacturing Techniques for Adaptive Coastline Protection Structures. *Buildings* **2022**, *12*, 1806, https://doi.org/10.3390/buildings12111806.
9. *DIN EN 1992-1-1:2011-01, Eurocode_2: Bemessung und Konstruktion von Stahlbeton- und Spannbetontragwerken_- Teil_1-1: Allgemeine Bemessungsregeln und Regeln für den Hochbau; Deutsche Fassung EN_1992-1-1:2004_+ AC:2010*; Beuth Verlag GmbH: Berlin, https://dx.doi.org/10.31030/1723945.
10. Kloft, H.; Krauss, H.-W.; Hack, N.; Herrmann, E.; Neudecker, S.; Varady, P.A.; Lowke, D. Influence of process parameters on the interlayer bond strength of concrete elements additive manufactured by Shotcrete 3D Printing (SC3DP). *Cement and Concrete Research* **2020**, *134*, 106078, https://doi.org/10.1016/j.cemconres.2020.106078.
11. Dreßler, I.; Freund, N.; Lowke, D. The Effect of Accelerator Dosage on Fresh Concrete Properties and on Interlayer Strength in Shotcrete 3D Printing. *Materials Journal, Special Issue "Concrete 3D Printing and Digitally-Aided Fabrication"* **2020**, https://doi.org/10.3390/ma13020374.
12. *DIN EN 14488-2:2006-09, Prüfung von Spritzbeton_- Teil_2: Druckfestigkeit von jungem Spritzbeton; Deutsche Fassung EN_14488-2:2006*; Beuth Verlag GmbH: Berlin, https://dx.doi.org/10.31030/9710986.
13. Lootens, D.; Jousset, P.; Martinie, L.; Roussel, N.; Flatt, R.J. Yield stress during setting of cement pastes from penetration tests. *Cement and Concrete Research* **2009**, *39*, 401–408, https://doi.org/10.1016/j.cemconres.2009.01.012.
14. Hack, N.; Kloft, H. Shotcrete 3D Printing Technology for the Fabrication of Slender Fully Reinforced Freeform Concrete Elements with High Surface Quality: A Real-Scale Demonstrator. In *Second RILEM International Conference on Concrete and Digital Fabrication*; Bos, F.P., Lucas, S.S., Wolfs, R.J., Salet, T.A., Eds.: Springer International Publishing: Cham, 2020, pp. 1128–1137, https://doi.org/10.1007/978-3-030-49916-7_107.
15. Maboudi, M.; Gerke, M.; Hack, N.; Brohmann, L.; Schwerdtner, P.; Placzek, G. Current Surveying Methods for the Integration of Additive Manufacturing in the Construction

Process. In *The International Archives of the Photogrammetry, Remote Sensing and Spatial Information Sciences*, Volume XLIII-B4-2020, 2020 https://doi.org/10.5194/isprs-archives-XLIII-B4-2020-763-2020.

16. Lachmayer, L.; Dörrie, R.; Kloft, H.; Raatz, A. Process Control for Additive Manufacturing of Concrete Components. In *Third RILEM International Conference on Concrete and Digital Fabrication*; Buswell, R., Blanco, A., Cavalaro, S., Kinnell, P., Eds.: Springer International Publishing: Cham, 2022, pp. 351–356, https://doi.org/10.1007/978-3-031-06116-5_52.